A Fully-coupled Thermo-Hydro-Mechanical Model for the Description of the Behavior of Swelling Porous Media

Hanifi Missoum, Nadia Laredj, Karim Bendani, Mustapha Maliki

Construction, Transport and Protection of the Environment Laboratory (LCTPE)
Université Abdelhamid Ibn Badis de Mostaganem, Algeria
hanifimissoum@yahoo.fr, nad27000@yahoo.fr, bendanik@yahoo.fr, mus27000@yahoo.fr

Abstract: Although many numerical models have been proposed for unsaturated porous media, unrealistic assumptions have been made, such as the non-deformable nature of media, constant material properties, the neglecting of convection heat flow transfer, and static air phase. Most of these conditions are not justifiable for porous media with low hydraulic permeability and high swelling activity. In the present article, a fully coupled thermo-hydro-mechanical model is proposed that takes into account nonlinear behavior, including both the effects of temperature on dynamic viscosity of liquid water and air phase, and the influence of temperature gradient on liquid and air flows. Fully coupled, nonlinear partial differential equations are established and then solved by using a Galerkin weighted residual approach in space domain and an implicit integrating scheme in time domain. The obtained model is finally validated by means of some case tests for the prediction of the thermo-hydro-mechanical behaviour of unsaturated swelling soils.

Keywords: multiphase flow; water transfer; unsaturated porous media; finite element; conservation; simulation

1 Introduction

Swelling porous materials are commonly found in nature as well as developed in industry. They are studied in many disparate fields including in soil science, in hydrology, in forestry, in geotechnical, chemical and mechanical engineering, in condensed matter physics, in colloid chemistry and in medicine. This article specifically focuses on unsaturated swelling clays, which are widely distributed in nature. In agriculture, water adsorption by the clay determines the ability of soils to transport and supply water and nutrients. Compacted bentonites play a critical role in various high level nuclear waste isolation scenarios and in barriers for

commercial landfills [1, 2]. In engineering and construction, swelling and compaction of clayey soils induce stresses which are very troublesome in foundation and structure buildings.

The engineering behaviour of unsaturated soil has been the subject of numerous experimental and theoretical investigations [3-8]. Numerous researches have been undertaken on both the experimental and theoretical aspects of thermo-hydro-mechanical transfer processes in porous media. Firstly, many of those studies have analysed the coupling behaviour on saturated media [9-11] based on Biot theory. Some of these investigations were founded on small temperature gradients assumptions and non-convective heat flow; further, no phase fluid change was taken into account and the physical material properties were constant.

Finite element solutions for non-isothermal two phase flows of deformable porous media were developed by [12], where the pore-air pressure is atmospheric condition [13]. In most of the studies [9-12], temperature effect on dynamic viscosity and permeability were neglected.

In the present article, a fully coupled thermo-hydro-mechanical model is proposed, which takes into account nonlinear behaviour, including the effects of temperature on the dynamic viscosity of both liquid water and air phases, as well as the influence of temperature gradient on liquid and air flows. The fully coupled, nonlinear partial differential equations are established and then solved by using a Galerkin weighted residual approach in space domain and an implicit integrating scheme in time domain. The obtained model has been finally validated by means of some case tests for the prediction of the thermo-hydro-mechanical behaviour of unsaturated swelling soils.

2 Theoretical Formulation

In this work a three-phase porous material consisting of solid, liquid and air requires consideration. A set of coupled governing differential equations are presented below to describe coupled multiphase flow in the soil. The model is based on combinations of equations or derivations from conservation principles and the classical laws of known physical phenomena for the coupled flow. Governing differential equations for pore water, pore air and heat transfer in unsaturated soil are derived as follows:

2.1 Heat Transfer

Considering heat transfer by means of conduction, convection and latent heat of vaporization effects, and applying the principle of conservation of energy, the following equation is derived:

$$\frac{\partial \phi}{\partial t} = -\nabla . Q \tag{1}$$

Where ϕ is the heat content of the soil and Q is the total heat flux, defined as:

$$\begin{aligned} Q = &-\lambda_T \nabla T - \left(v_v \rho_v + v_a \rho_v\right) L + \\ &\left(C_{pl} v_l \rho_l + C_{pv} v_v \rho_l + C_{pv} v_a \rho_v + C_{pda} v_a \rho_{da}\right)\left(T - T_r\right) \end{aligned} \tag{2}$$

$$\phi = H_c \left(T - T_r\right) + L n S_a \rho_v \tag{3}$$

where H_c is the specific heat capacity of the soil, T is the temperature, T_r is the reference temperature, L is the latent heat of vaporization of soil water, C_{pl}, C_{pv} and C_{pa} are the specific heat capacity of soil water, soil vapour and soil dry air respectively and λ_T is the coefficient of thermal conductivity of the soil.

Three modes of heat transfer are included: thermal conduction, sensible heat transfer associated with liquid, vapour and air flow and latent heat flow with vapour.

2.2 Moisture Transfer

For the moisture transfer, the mass transfer balance equation, accommodating both liquid and vapour, can be expressed as:

$$\frac{\partial(\rho_l n S_l)}{\partial t} + \frac{\partial(\rho_v n(S_l - 1))}{\partial t} = -\rho_l \nabla . v_l - \rho_l \nabla . v_v - \rho_v \nabla . v_a \tag{4}$$

where n is the porosity, ρ is the density, S_l is the degree of saturation, t is time and v the velocity. The subscripts l, a and v refer to liquid, air and water vapour respectively.

In this simulation, a generalized Darcy's law is used to describe the velocities of pore water and air:

$$v_l = -\frac{K_l}{\gamma_l}(\nabla u_l + \gamma_l \nabla z) \tag{5}$$

$$v_a = -K_a \nabla\left(\frac{u_a}{\gamma_a}\right) \tag{6}$$

where K_l and K_a are the hydraulic conductivities of liquid and air, respectively, γ_l is the unit weight of liquid, γ_a is the unit weight of air, u_l is the pore water pressure, u_a is the pore air pressure, z is the elevation and ∇ is the gradient operator.

The hydraulic conductivities of water and air through soil may be expressed in terms of the saturation degree or water content as follows:

$$K_l = K_l(S_l) \tag{7}$$

$$K_a = K_a(S_l, \eta_a) \tag{8}$$

where η_a is the dynamic viscosity of air.

The water vapour density ρ_v is evaluated from the thermodynamic assumptions, and when liquid and vapour phases are in equilibrium, it can be evaluated by the following relationship [14]:

$$\rho_v = \rho_0 . h_t \tag{9}$$

where h_t is the total relative humidity calculated by the following expression:

$$h_t = \exp\left(\frac{u_l - u_a}{\rho_l R_v T}\right) \tag{10}$$

and ρ_0 is the total saturated water vapour defined as [14]:

$$\rho_0 = \left[194.4 \exp\left(-0.06374(T-273) + 0.1634.10^3 (T-273)^2\right)\right]^{-1} \tag{11}$$

R_v is the gas constant for water vapour end *T* is the temperature.

2.3 Pore Air Mass Transfer

Using Henry's law to take account of dissolved air in the pore water, the following equation is derived for the dry air phase from the principle of mass conservation:

$$\frac{\partial\left[n\rho_a(S_a + HS_l)\right]}{\partial t} = -\nabla.\left[\rho_a(v_a + Hv_l)\right] \tag{12}$$

where, H is Henry's volumetric coefficient of solubility and ρ_a is the dry air density.

The dry air density ρ_a can be evaluated from Dalton's law as:

$$\rho_a = \frac{u_a}{RT} - \frac{R_v}{R}\rho_v \tag{13}$$

R and R_v are the gas constants for dry air and water vapour respectively, and T is the temperature.

2.4 Constitutive Stress-Strain Relationship

For problems in unsaturated swelling porous media, the total strain ε is assumed to consist of components due to suction, temperature and stress changes. This can be given in an incremental form as:

$$d\varepsilon = d\varepsilon_\sigma + d\varepsilon_s + d\varepsilon_T \tag{14}$$

where the subscripts σ, s and T refer to net stress, suction and temperature contributions.

The stress-strain relationship can therefore be expressed as:

$$d\sigma'' = D(d\varepsilon - d\varepsilon_s - d\varepsilon_T) \tag{15}$$

where

$$[\sigma''] = [\sigma_x \;\; \sigma_y \;\; \sigma_z \;\; \tau_{xy} \;\; \tau_{yz} \;\; \tau_{xz}] \tag{16}$$

where σ'' is the net stress and D is the elastic matrix. A number of constitutive relationships can be employed, for example an elasto-plastic constitutive relationship [15].

2.5 Coupled Equations

This leads to a set of coupled, nonlinear differential equations, which can be expressed in terms of the primary variables T, u_l, u_a and u of the model as energy balance:

$$\begin{aligned} C_{Tl}\frac{\partial u_l}{\partial t} + C_{TT}\frac{\partial T}{\partial t} + C_{Ta}\frac{\partial u_a}{\partial t} + C_{Tu}\frac{\partial u}{\partial t} \\ = \nabla[K_{Tl}\nabla u_l] + [K_{TT}\nabla T] + [K_{Ta}\nabla u_a] + J_T \end{aligned} \tag{17}$$

Mass balance:

$$\begin{aligned} C_{ll}\frac{\partial u_l}{\partial t} + C_{lT}\frac{\partial T}{\partial t} + C_{la}\frac{\partial u_a}{\partial t} + C_{lu}\frac{\partial u}{\partial t} \\ = \nabla[K_{ll}\nabla u_l] + [K_{lT}\nabla T] + [K_{la}\nabla u_a] + J_l \end{aligned} \tag{18}$$

$$C_{al}\frac{\partial u_l}{\partial t} + C_{aT}\frac{\partial T}{\partial t} + C_{aa}\frac{\partial u_a}{\partial t} + C_{au}\frac{\partial u}{\partial t} = \nabla[K_{al}\nabla u_l] + [K_{aa}\nabla u_a] + J_a \tag{19}$$

Stress equilibrium:

$$C_{ul}du_l + C_{uT}du_T + C_{ua}du_a + C_{uu}du + db = 0 \tag{20}$$

where K_{ij} and C_{ij} represent the corresponding terms of the governing equations ($i, j = l, T, a, u$)

3 Discretisation Techniques

The numerical solution of the theoretical models commonly used in geo-environmental problems is often achieved by a combination of numerical discretisation techniques. For the example presented in this paper, the finite element method is employed for the spatial discretisation and a finite difference time stepping scheme for temporal discretisation.

In particular, the Galerkin weighted residual method [16] is used to formulate the finite element discretisation. An implicit mid-interval backward difference algorithm is implemented to achieve temporal discretisation since it has been found to provide a stable solution for highly non-linear problems [17]. With appropriate initial and boundary conditions the set of typically nonlinear coupled partial differential equations can be solved.

Applying a Galerkin formulation of the finite element method, we obtain a system of matrix equations are as follows:

$$[K]\{\varphi\}+[C]\{\dot{\varphi}\}+\{J\}=0 \tag{21}$$

where

$$[K]=\begin{bmatrix} K_{TT} & K_{Tl} & K_{Ta} & 0 \\ K_{lT} & K_{ll} & K_{la} & 0 \\ 0 & K_{al} & K_{aa} & 0 \\ 0 & 0 & 0 & 0 \end{bmatrix},\ [C]=\begin{bmatrix} C_{TT} & C_{Tl} & C_{Ta} & C_{Tu} \\ C_{lT} & C_{ll} & C_{la} & C_{lu} \\ C_{aT} & C_{aL} & C_{aa} & C_{au} \\ C_{uT} & C_{ul} & C_{ua} & C_{uu} \end{bmatrix} \tag{22}$$

$$\{\varphi\}=\begin{pmatrix} T & u_l & u_a & u \end{pmatrix}^T,\ \{\dot{\varphi}\}=\begin{pmatrix} \frac{dT}{dt} & \frac{du_l}{dt} & \frac{du_a}{dt} & \frac{du}{dt} \end{pmatrix}^T,$$

$$\{J\}=\begin{pmatrix} J_T & J_l & J_a & J_u \end{pmatrix}^T \tag{23}$$

To solve equation (21), a general form of fully implicit mid-interval backward difference time stepping algorithm is used to discretise the governing equation temporally. Therefore equation (21) can be rewritten as:

$$K\left(\varphi^n\right)\left[1-\theta\right]\left\{\varphi^{n+1}\right\}+\theta\left\{\varphi^n\right\}+C\left(\varphi^n\right)\left[\frac{\left\{\varphi^{n+1}\right\}-\left\{\varphi^n\right\}}{\Delta t}\right]+J\left(\varphi^n\right)=\{0\} \tag{24}$$

$\left(\varphi^n\right)$ is the level of time at which the matrices *K*, *C* and *J* are to be evaluated and is given by:

$$\left(\varphi^n\right)=\omega\left\{\varphi^{n+1}\right\}+(1-\omega)\left\{\varphi^n\right\} \tag{25}$$

where ω is integration factor, which defines the required time interval ($\omega \in [0,1]$) and $\theta = 0, 0.5, 1$ for backward, central and forward difference schemes, respectively.

For a mid-interval backward difference scheme, $\omega = 0.5$ and $\theta = 0$. Therefore, equation (24) reduces to:

$$K\left(\frac{\{\varphi^{n+1}\}+\{\varphi^{n}\}}{2}\right)\{\varphi^{n+1}\}+C\left(\frac{\{\varphi^{n+1}\}+\{\varphi^{n}\}}{2}\right)\left(\frac{\{\varphi^{n+1}\}-\{\varphi^{n}\}}{\Delta t}\right) + J\left(\frac{\{\varphi^{n+1}\}+\{\varphi^{n}\}}{2}\right)=\{0\} \tag{26}$$

Eq. (26) may be rewritten in alternate form as:

$$K^{n+0.5}\{\varphi^{n+1}\}+C^{n+0.5}\left(\frac{\{\varphi^{n+1}\}-\{\varphi^{n}\}}{\Delta t}\right)+J^{n+0.5}=\{0\} \tag{27}$$

A solution for $\{\varphi^{n+1}\}$ can be obtained provided the matrices *K, C* and *J* at time interval ($n+0.5$) can be determined. This is achieved by the use of a predictor-corrector iterative solution procedure.

4 Applications and Results

4.1 Example 1

4.1.1 Problem Definition

The following example is investigated to demonstrate swelling pressure calculation by using the back hydro-mechanical model. The simulation begins with isothermal two phase flow coupled with deformation. Free extension is allowed at the first stage to calculate the free extension displacement on the boundary. The geometric set-up and boundary conditions are as shown in Fig. 1. The example is a compacted bentonite block, 0.025 m length and 0.024 m height. The element discretization is $\Delta x = 0.00125\,m$ and $\Delta y = 0.00124\,m$, eight nodded composed elements. The initial conditions of the system are: atmospheric air pressure and liquid saturation $S_l = 0.357$. A water solution enters the sample from the bottom under pressure described by the curve in Fig. 2. The corresponding part on the boundary is fully saturated.

The material properties for this example are based on data in the literature [18, 1] and summarized in Table 1. The deformation under free extension conditions is assumed to be non-linear elastic.

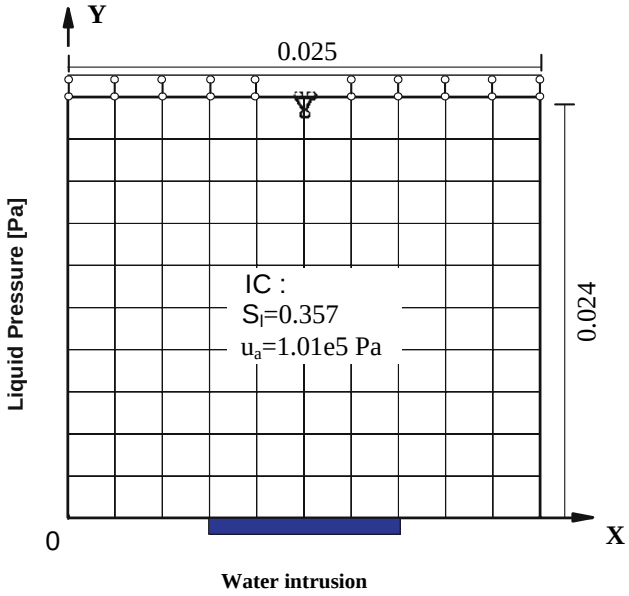

Figure 1
Model set-up of the example

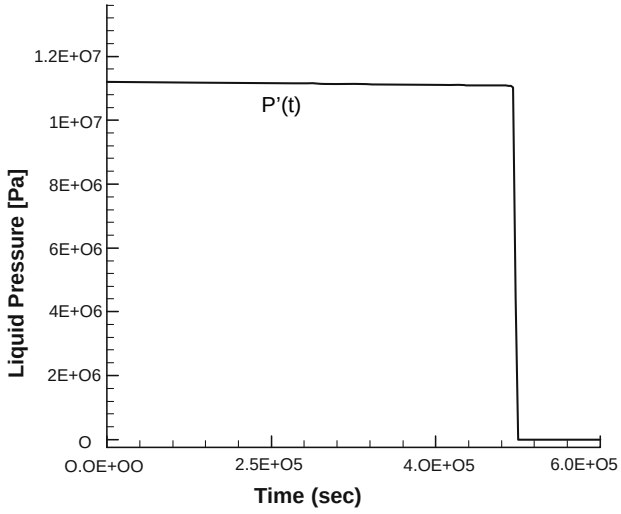

Figure 2
Curve of the liquid pressure on the boundary

Symbols	functions and constants	Units
ρ_l	1000	Kg/m^3
ρ_g	1.26	Kg/m^3
ρ_s	1600	Kg/m^3
S_l	$1-0.85\left[1-\exp\left(-1.20\times10^{-7}\left(u_a-u_l\right)\right)\right]$	
μ_l	1.20×10^{-3}	Pa s
μ_g	1.80×10^{-5}	Pa s
K_l	$\frac{1.2\times10^{-12}}{\mu_l[1+1.3\times10^{-10}\left(u_a-u_l\right)^{1.7}]}$	m/s
K_a	$1.3\times10^{-19}\frac{\gamma_a}{\mu_a}\left[e\left(1-S_l\right)\right]^{3.0}$	m/s
n	0.37	
S_0	31.80	m^2/g
E	3.5	MPa
ν	0.3	
T_r	293	°K

Table 1
Porous medium properties [18, 19]

4.1.2 Results and Discussion

The simulation results of the free extension processes after $5.8\times10^5\,s$ (6.7 days) are shown in Figs. 3 and 4. With the intrusion of water from the bottom, the saturation process starts. This phenomenon can clearly be seen from the saturation evolution profile along the vertical symmetric axis (Fig. 3). At the early stage, the value of liquid saturation increases quite fast. After $4.9\times10^5\,s$ (5.7 days) the liquid pressure on the bottom sinks at $5.0\times10^5\,s$ (5.8 days) reaches zero. Because of the low permeability of bentonite, the liquid pressure at the centre of the specimen sinks slower, which results in the higher pressure region in the specimen after 6.7 days as shown in Fig. 4a.

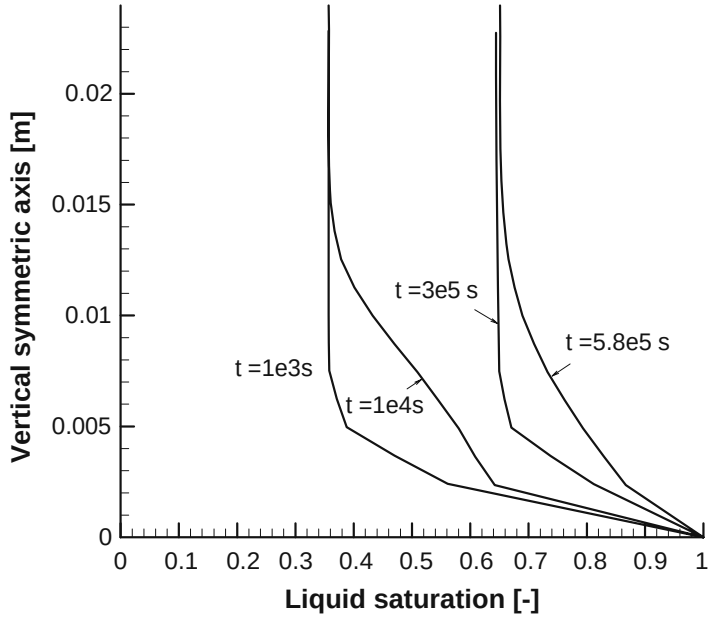

Figure 3
Computed profiles of liquid saturation along the vertical symmetric axis

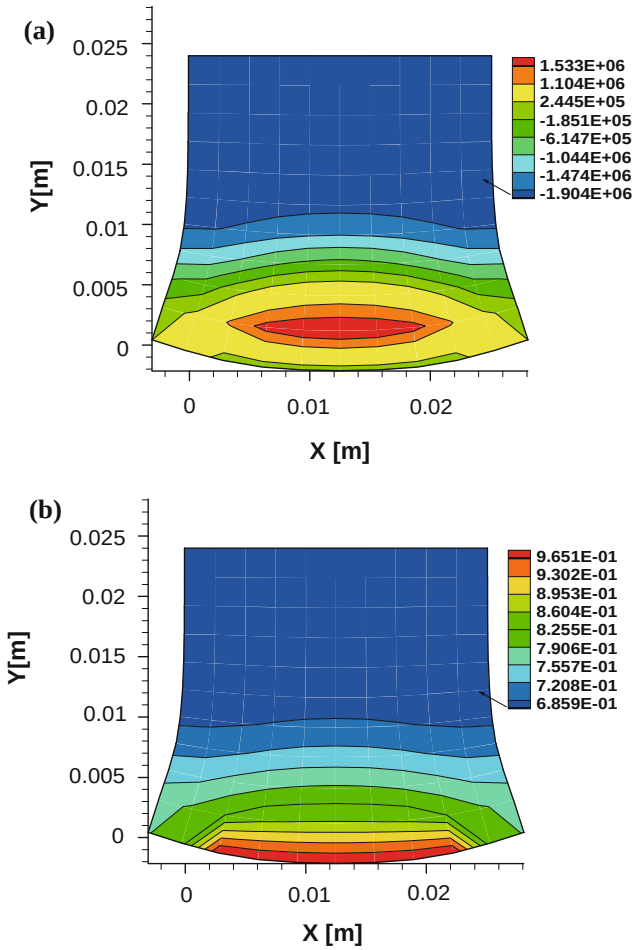

Figure 4
Simulation results of the free extension process
(a) Distribution of liquid pressure, (b) Distribution of liquid saturation

With the intrusion of water, the sample begins to expand. After 6.7 days, the shape of the specimen should be as shown in Fig. 5. The maximal width of the specimen increases about 20% (Fig. 5). In this example, experimental data from free swelling tests for compacted bentonites were used [18].

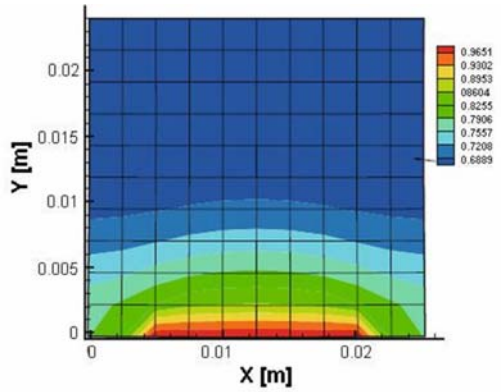

Figure 5
Simulated shape of the sample, and distribution of liquid saturation for material at $t = 5.8 \times 10^5$ s

4.2 Example 2

4.2.1 Problem Definition

The model has been verified through simulating a test problem of bentonite tested in laboratory conditions [20]. The compacted bentonite was planned to be used to limit the flow velocity of groundwater in the near field of a geological repository for radioactive waste. The sample of bentonite has a height of 203 mm. To minimize heat losses, the cell was insulated with a heat-proof envelope. Heat was applied at the bottom plate of the cylinder while the temperature at the other end was kept constant and equal to 20°c. A maximum temperature of 150° was applied. A constant water pressure was applied to the end opposite the one where the temperature variation was prescribed. Constant volume conditions were ensured in the test. The main variables that were measured during the test include temperature, relative humidity and total axial stress. The model geometry is the same as the sample with the height equal to 203 mm. The temperature variation at the bottom end of the model is as specified during the test; it was raised in steps until reaching 150°c. The temperature at the top end of the specimen was kept constant at 20°c. The other surfaces are adiabatic.

According to the test procedure, the hydraulic boundary condition is impermeable for all surfaces of the model. The gas pressure is equal to the atmospheric pressure. The initial value of porosity is 0.3242, initial temperature is 20°c, initial gas pressure is 0.10132 MPa and the initial stress of sample is 0.5 MPa. The initial values were obtained according to the measured data from the experiments [19].

According to the measured data from the bentonite [20, 21, 22], the intrinsic permeability is 1.0E-21 m^2 and the specific heat capacity of solids is 920 J/Kg.

4.2.2 Results and Discussion

Fig. 6 shows the comparison between measured temperatures as a function of time. At the bottom end of the sample, the measured and simulated temperatures agree well. At the top end of the sample, the simulation underestimates the temperature slightly at the initial heating stage, but trends generally agree well.

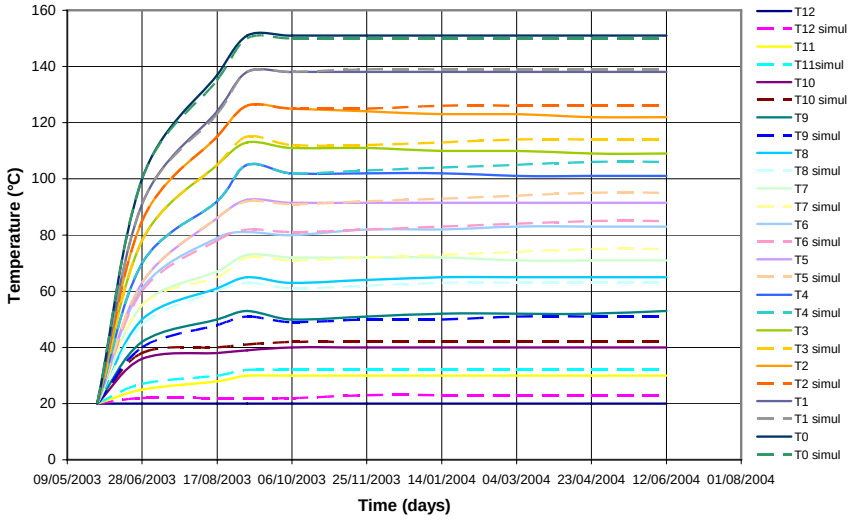

Figure 6
Comparison of results between the simulated and measured temperature at different locations (heights) of the sample as function of time

The good agreement between the simulated and measured temperatures indicates that the model can simulate the thermal response of processes having high temperature gradients. Numerical simulation shows that the thermal conductivity of bentonite, treated as a multiphase material, plays an important role in the thermal response of the whole medium. The numerical results can be further improved if the effects of the material heterogeneity can be quantified during testing.

The simulated results of the vapour pressure are shown in Fig. 7. Although there are no measured results with which to compare, it shows that the variation of vapour pressures is realistic.

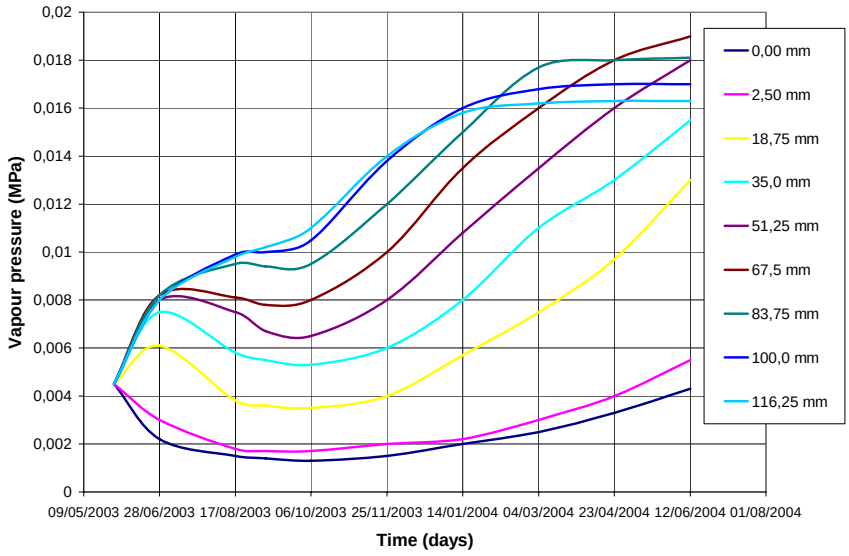

Figure 7
The simulated results of vapour pressure

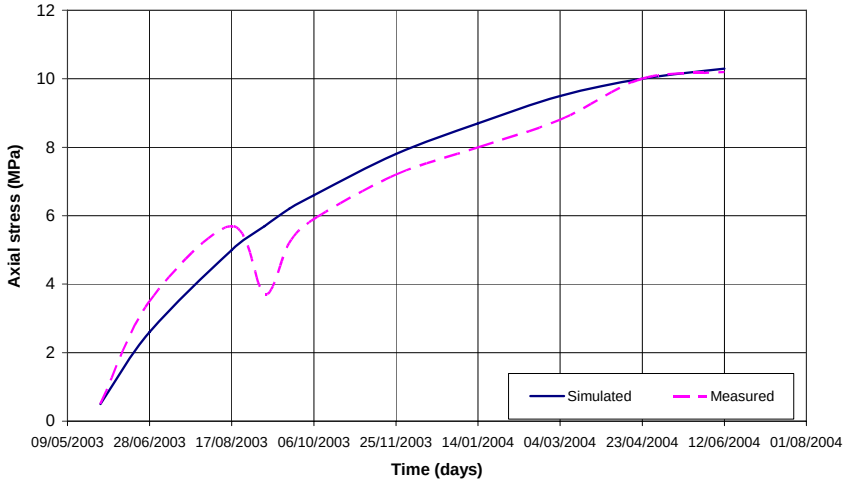

Figure 8
Comparison of results between simulated and measured axial stress

The evolution of the axial stress was also reasonably well simulated (Fig. 8), in trend and magnitude. Numerical calculation shows the results of stress strongly depend on the constitutive relationship between stress and strain. More comprehensive development of the material models is needed to further improve the numerical capability of the code, such as elastoplastic models for example.

Conclusion

A fully coupled thermo-hydro-mechanical model is proposed, which takes into account nonlinear behaviour including the effects of temperature on dynamic viscosity of both liquid water and air phases, and the influence of temperature gradient on liquid and air flows. A set of fully coupled, nonlinear partial differential equations were established and then solved by using a Galerkin weighted residual approach in the space domain and using an implicit integrating scheme in time domain. A range of simulation results has been presented detailing the hydraulic and thermal behaviour of expansive soil. The simulation results have been compared with the experimentally measured results and it was shown that a good correlation was found in the hydraulic regime and a reasonable correlation in the thermal field. The results of the validations indicate that the model is general and suitable for the analyses of many different problems in unsaturated soils.

References

[1] Gens A, Olivella S: Chemo-Mechanical Modelling of Expansive Materials. 6th International Workshop on Key Issues in Waste Isolation Research. Paris (France), 2001, pp. 463-495

[2] Andra : Dossier argile. Evaluation de la faisabilité du stockage géologique en formation argileuse, Rapport Andra C.RP.ADP.04.0002,2005

[3] Fredlund DG, Morgenstern NR: Stress State Variables for Unsaturated Soils. J. Geotch. Engng. Div., ASCE 103, 1977, pp. 447-466

[4] Alonso EE, Gens A, Josa A: A Constitutive Model for Partially Saturated Soils. Geotechnique 40, 1990, pp. 405-430

[5] Cui J, Delage P: Yielding and Plastic Behaviour of an Unsaturated Compacted Silt. Geotechnique, 1996, 46 (2): pp. 291-311

[6] Cui YJ, Yahia-Aissa M, Delage P: A Model for the Volume Change Behaviour of Heavily Compacted Swelling Clays. Engineering Geology, 2002, 64 (2): pp. 233-250

[7] Fleureau JM, Verbrugge JC, Huergo PJ, Correia AG, Kheirbek Saoud S: Aspects of the Behaviour of Compacted Clayey Soils on Drying and Wetting Paths. Can. Geotech. Engng., 2002, 39: pp. 1341-1357

[8] Saiyouri N, Tessier D, Hicher PY: Experimental Study of Swelling in Unsaturated Compacted Clay. Clay minerals, 2004, 39 (4): pp. 469-479

[9] Detournay E, Cheng A H D: Poroelastic Response of a Borehole in a Non-Hydrostatic Stress Field, International Journal of Rock Mechanics and Mining sciences and Geomechanics Abstracts, 1988, 25 (3): pp. 171-182

[10] Cheng A H D, Abousleiman Y, Roegiers J C: Review of Some Poroelatic Effects in Rock Mechanics. International Journal of Rock Mechanics and Mining Sciences and Geomechanics Abstracts, 1993, 30 (7): pp. 1119-1126

[11] Senjuntichai T: Green's Functions for Multi-layered Poroelastic Media and an Indirect Boundary Element Method, PhD Thesis. Winnipeg: University of Manitoba, 1994

[12] Britto A M, Savvidou C, Gunn M J: Finite Element Analysis of the Coupled Heat Flow and Consolidation around Hot BURIED objects. Soils and Foundations, 1992, 32 (1): pp. 13-25

[13] Chen W, Tan X, Yu H, Jia S: A Fully Coupled Thermo-Hydro-Mechanical Model for Unsaturated Porous Media. Journal of Rock Mechanics and Geotechnical Engineering, 2009, 1 (1): pp. 31-40

[14] Edlefsen NE, Anderson ABC: The Thermodynamics of Soil Moisture Hilgardia, 1943, pp. 31-299

[15] Thomas HR, He H: Modelling the Behaviour of Unsaturated Soil Using an Elastoplastic Constitutive Relationship. Geotechnique, 1998, 48 (5): pp. 589-603

[16] Zienkiewicz OC, Taylor RL: The Finite Element Method. Butterworth-Heinemann, 5th ed., Oxford, 2000

[17] Thomas HR, King SD: Simulation of Fluid Flow and Energy Processes Associated with High Level Radioactive Waste Disposal in Unsaturated Alluvium. Water Ressour. Res., 1991, 22 (5): pp. 765-775

[18] Agus S, Schanz T: Swelling Pressures and Wetting-Drying Curves of a Highly Compacted Bentonite-Sand Mixture, in: Schanz T (2003) Unsaturated Soils: Experimental Studies, Proceedings of the International Conference. From Experimental Evidence Towards Numerical Modelling of Unsaturated Soils. Weimar, Germany, September 18-19, 2003, Volume 1 Series: Springer Proceedings in Physics (93) Volume Package: Unsaturated Soils: Experimental Studies 2005, XIV, p. 533, Springer

[19] Poling BE, Prausnitz JM, O'Connell JP: The Properties of Gases and Liquids, Mc Graw Hill, 5th ed., New York, 2001

[20] Gatabin C, Billaud P: Bentonite THM mock up experiments. Sensor data report. CEA, Report NT-DPC/SCCME 05-300-A, 2005

[21] Loret B, Khalili N: A three phase model for unsaturated soils. Int. J. Numer. Anal. Meth. Geomech; 2000, 24: pp. 893-927

[22] Marshall TJ, Holmes JW: Soil physics. Bristol. Cambridge University Press, 2nd ed., New York, 1988